Journal of Heat and Mass Transfer Research 12 (2025), Serial Number 24, 323 – 333

Semnan University

Journal of Heat and Mass Transfer Research

Journal homepage: https://jhmtr.semnan.ac.ir

ISSN: 2383-3068

Research Article

Experimental Investigation of Minimum Fluidization Velocity and Pressure Drop in Fluidized Bed of Teff Grain

Lemi Demissie Boset [a] *, Zewdu Abdi Debele [b], Amana Wako Koroso [a]

[a] *School of Mechanical, Chemical, and Material Engineering, Adama Science and Technology University, Adama, Oromia, 0000, Ethiopia*

[b] *Faculty of Agriculture, University of Eswatini, Luyengo, Eswatini, M205, Eswatini*

ARTICLE INFO

Article history:

Received: 2024-11-05

Revised: 2025-03-26

Accepted: 2025-04-27

Keywords:

Minimum fluidization velocity;

Pressure drop;

Pneumatic conveyor;

Drying;

Teff grain.

ABSTRACT

Gas-fluidization characteristics of teff grain are crucial for understanding its behavior under gas flow, enabling it to act like a fluid, which is vital for pneumatic conveying systems. Key parameters include the minimum fluidization velocity and the pressure drop across the fluidized bed, which reflect the interaction between gas and grains. These characteristics are essential for selecting the appropriate phase of the pneumatic conveying system, ultimately improving the processing and handling of teff grain. Air retention capabilities are significant indicators of a material's suitability for dense-phase conveying. Gas fluidized bed tests were performed to evaluate the bulk flow behavior of teff grain for both dilute and dense-phase pneumatic conveyors. Results indicated that teff grain has poor air retention, evidenced by bubble formation at low airflow rates, suggesting it is more suitable for dilute-phase conveying. Experiments measured the minimum fluidization air velocity and pressure drop per bed height using a CEL-MKII apparatus at various airflow rates. Experimental studies revealed that bubbles form in the fluidized bed at the minimum superficial gas velocity, with a pressure drop ranging between 100 mbar/m and 107 mbar/m and a minimum fluidization velocity of 0.56 m/s and 0.575 m/s. These findings guide the design of effective drying and pneumatic conveying systems for teff grain.

1. Introduction

Teff is an important cereal crop indigenous to Ethiopia, where major varieties can also be found. It is a gluten-free grain with highly regarded nutritional benefits and has recently attracted the attention of the modern food business.

However, there isn't adequate information available on its handling and processing characteristics because it's a relatively new raw material for modern industry [1]. In Ethiopia, Teff production, handling, and processing practices are dominated by traditional methods.

Traditional methods of production, handling, and processing lead to low yields and significant losses. Teff grass has unique characteristics, including a short panicle, high lodging tendency, and weak stem, which complicate harvesting and threshing. Moreover, small grain size makes

* **Corresponding author.**
E-mail address: lemi.demissie@astu.edu.et

Cite this article as:

Demissie Boset, L. D., Abdi Debele, Z. and Wako Koroso, A., 2025. Experimental Investigation of Minimum Fluidization Velocity and Pressure Drop in Fluidized Bed of Teff Grain. *Journal of Heat and Mass Transfer Research*, 12(2), pp. 323-333.
https://doi.org/10.22075/JHMTR.2025.35810.1632

handling challenging, leading to significant losses, as pre- and post-harvest losses account for around 40% of yield loss in teff, according to information gathered from the farmers [2].

Broadcasting of teff seed by hand uses a rate of 25–50 kg per hectare, and researchers approved reducing the seed rate to between 2.5 and 3 kg per hectare. Teff faces substantial losses of 16-30% during harvesting and post-harvest stages, largely due to issues such as shattering and contamination where lodging contributes to the yield loss of up to 30% [3]. Teff post-harvest losses in the most common pathway of the rural-urban value chain range from 2.2 to 3.3 percent of the total collected amounts. These amounts can vary depending on the storage facilities used and the expected transportation losses at the farm. This is the reason why our country produces low-yield and low-quality teff [4].

Most researchers mention that it is difficult to handle Teff grain without loss because of its size. The engineering discipline of bulk material handling is focused on designing machinery for the handling of dry materials. Dry bulk materials are powdery, granular, or lumpy and are stored in heaps. Minerals, ores, coal, grains, wood chips, sand, gravel, clay, cement, ash, salt, chemicals, and loose bulk forms of grain, sugar, flour, and stone are a few examples of dry bulk materials. It may also have to do with managing mixed waste. Any industry that processes bulk ingredients, such as those in the food, beverage, confectionery, pet food, animal feed, tobacco, chemical, agricultural, polymer, plastic, rubber, ceramic, electronics, metals, minerals, paint, paper, textiles, and more categories, needs bulk material handling [5]. During the study, rational conditions for the drying process were determined. Investigating fluidized bed drying of the extract from callus cultures makes it possible to acquire extracts containing more physiologically active ingredients.

Karimi et al. [6] investigated the suitability of SFBD for drying other materials; the current study may be modified for use with additional heat-sensitive food materials with varying particle sizes. Other fluidized bed applications, such as mixing, may also be suited for the multi-angle whirling distributors and combustion in future research.

Pontawe et al. [7] The study's conclusions showed that the participants followed the recommended protocols for managing and using the PHilMech Fluidized Bed Dryer, using clear, concise, comprehensible, and legally binding operational policies and procedures. Since farmers, especially those who are introducing machinery, needed to build new competencies, the majority of them have internalized the knowledge they have gained through many training sessions. They examined how various treatments affected the lowering of phytic acid contents in dehulled faba beans. Three different procedures were used: soaking, microwaving, and fluidized bed drying. It appears that thermal treatment had minimal influence on phytic acid levels because fluidized bed drying did not significantly lower the concentration of phytic acid from faba beans. Phytic acid levels in the faba beans were somewhat lowered by soaking, but the effect of microwaving was greater [8]. The most popular method for drying solids is using a gas-solid fluidized bed. The exceptional solid mixing properties of fluidized beds result in the high heat and mass transmission rates that are required. Because of the high latent heat of vaporization, solid drying is an extremely energy-intensive process; hence, these high transfer rates are essential [9]. By improving the airflow distribution using simulation calculations, the granulator's overall performance was raised, which increased drying efficiency and decreased energy usage. Additionally, a thorough comprehension of the intricate airflow patterns and turbulence properties inside the granulator was acquired, making it easier to identify the variables influencing airflow homogeneity, such as the fish-scale hole structure's opening rates and structural layout [10].

In a moving bed mode of dense phase flow, powdered materials with excellent air retention qualities, such as fly ash, cement, and wheat, can typically be transported at moderate speeds. Large mono-sized particles with very good permeability, such as polyethylene pellets, can generally be conveyed at low velocities in a plug mode of dense phase flow [11]. For example, fly ash, cement, and flour are powdered materials that have excellent air retention qualities and can usually be transported at low speeds using a sliding bed mode of dense phase flow. Large mono-sized particles with very good permeability, such as polyethylene pellets, can generally be conveyed at low velocities in a plug mode of dense phase flow [12, 13].

Coarse granular materials with poor air retention and permeability, such as sand and alumina, are often only capable of being carried in dilute phase suspension flow in conventional pneumatic conveying systems, especially if they have a wide particle size distribution [14]. A new reactor concept for biomass gasification is the supercritical water fluidized bed. Experimental research on the hydrodynamics of a supercritical water-fluidized bed was carried out in this paper [15]. For temperatures ranging from 633 to 693 K and pressures ranging from 23 to 27 MPa, the frictional pressure drops of a fixed bed and a fluidized bed were measured [16].

In chemical engineering, fluidized bed apparatuses are extremely common. To understand and predict how these systems work, especially in gas-solid flows, a detailed understanding of the apparatus's fluid dynamics is essential [17].

A mathematical model simplifies the prediction of breakthrough curves in fixed-bed adsorption by ignoring radial dispersion and assuming constant interstitial velocity and porosity [18]. It also relies on a linear adsorption rate and describes the equilibrium relationship using the Langmuir isotherm. This allows for a simplified understanding of the adsorption process within the bed [19].

The lowest bubbling speed at which fluidized beds can function at elevated temperatures was investigated. In a 54 mm transparent column, fluidization, and collapse tests were conducted on silica sand and corundum samples at temperatures between 30 and 500°C. After fluidization, every solid under investigation which falls into group A of the Geldart classification showed uniform expansion at every temperature [20]. The minimum fluidization liquid velocity, U_{mf}, is the first obvious hydrodynamic parameter of primary relevance in the design of a three-phase fluidized bed. It is the minimal superficial liquid velocity that, when combined with a particular superficial gas velocity, causes particles in the bed to move from rest to motion [21]. The effects of heat and mass transfer parameters on the efficiency of fluidized bed drying have been investigated to improve the input and output conditions [22].

The experiment was carried out using two different materials, wheat and corn [23]. First and second laws of thermodynamics-based energy and exergy models are developed. Furthermore, certain unifying non-dimensional experimental correlations have been developed for estimating the efficiency of the fluidized bed drying process [24]. The constructed model was used to examine the impact of hydrodynamic and thermodynamic parameters such as inlet air temperature, starting moisture content, and well-known Fourier and Reynolds numbers on energy efficiency and energy efficiency. The model predictions, non-dimensional correlations, and available experimental results all agreed well [25]. When only AI was blasted, the pressure dropped and the power required rose as the air velocity increased. Wheat conveying had the largest pressure drop and power consumption, while sunflower conveying had the lowest pressure drop and power requirement. The pressure drop and power required to transport all seeds through a pipeline increased with air velocity and conveying capacity [26].

To achieve a nonhomogeneous drying outcome, a recirculating type solar dryer with a pneumatic conveyor will be used as the recirculating equipment. As the grains move through the pneumatic conveyor, quick heat and mass transfer occur, resulting in an even drying process and homogeneous drying results. A feed hopper, centrifugal blower, pneumatic conveyor, and a transparent structure operating as a drying chamber with a hopper with a vortex at the top compose the entire solar dryer [27]. A pneumatic conveyor was employed to recirculate the grain and execute the continuous drying operation.

Teff grain is classified under Geldart Group B, which includes materials that are typically categorized as free-flowing and exhibit fluidization behavior with distinct bubbling. Group B particles generally have a density and size range that allow them to fluidize easily with noticeable bubbling but without excessive cohesiveness or strong interparticle forces. This classification is essential in understanding the pneumatic conveying characteristics of teff, as it influences parameters such as minimum fluidization velocity, pressure drop, and particle-air interactions in conveying systems.

The small grain size complicates handling, and issues like lodging and shattering further contribute to losses. To address these challenges, bulk material handling and fluidized bed technologies offer potential solutions for improving drying, conveying, and processing efficiency. Studies on fluidized bed drying and pneumatic conveying demonstrate their effectiveness in enhancing airflow distribution, optimizing drying efficiency, and minimizing energy consumption. By integrating modern handling and drying technologies, Teff processing can be improved, reducing losses and ensuring better quality for industrial applications.

2. Materials and Methods

Teff varieties (DZ-Cr-442 RIL77C) and Boset (DZ-Cr-409) were obtained from Debre Zeit Agricultural Research Center of the Ethiopian Institute of Agricultural Research (EIAR). These teff varieties were released by the national teff improvement program of the Ethiopian Institute of Agricultural Research (EIAR) as shown in Figure 1.

The experiments were conducted at Adama Science and Technology University, Chemical Department laboratory. The experiments, such as those on physical properties and fluidized bed tests of two teff grain varieties at different moisture content, were conducted.

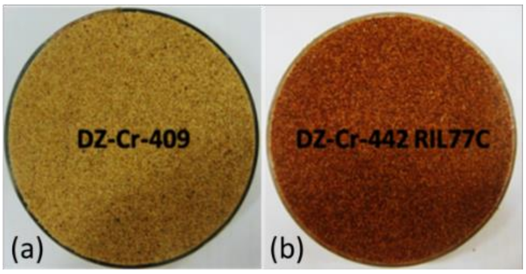

Fig. 1. Teff varieties (a) Boset (DZ-Cr-409) and (b) Felagot (DZ-Cr-442 RIL77C)

Teff grain moisture content (Boset and Felagot) was measured using the oven-drying method per ASAE standard S352.3 (ASAE, 1994). Approximately 160 grams of each sample were weighed wet weight and dried in an oven at 105 ± 2°C for at least 24 hours until a constant weight was achieved. After drying, the samples were cooled in a desiccator to room temperature, and the final weight was recorded. The moisture content was calculated based on the weight difference before and after drying. This process was repeated for multiple samples to ensure consistency. Moisture content is calculated using the following equation [28].

$$MC = \frac{(w-d)}{w} \times 100 \tag{1}$$

where MC is the moisture content (%), w is the weight while wet, and d is the weight while dry.

The measured moisture content for the two varieties of teff using the oven dry method is shown in Figure 2.

Fig. 2. Teff grain in the oven for moisture content measurement

To measure the weight of teff grain for determining moisture content, an electronic balance shown in Figure 3, with a precision of 0.01 g, was utilized, capable of handling weights up to 3kg, while laboratory ovens ranging in size from one cubic foot (28 liters) to 32 cubic feet (906 liters) were employed, with temperatures that can reach up to 300°C, ensuring accurate and efficient moisture measurement.

Fig. 3. Weighing teff grain using an electronic balance

The size of the teff grain was accurately determined using scanning electron microscopy, which provided high-resolution imaging and enabled precise measurements of its length, width, and thickness. These measurements were used to characterize the physical properties of the grain, revealing a wide range of dimensions. The smallest dimension recorded was 476 µm, while the largest was 1.1 mm, with intermediate sizes of 539 µm, 681 µm, 733 µm, 864 µm, 936 µm, and 1 mm, as illustrated in Figure 4, and Table 1. Additionally, the measured angles varied between 13° and 76°. This detailed data highlights the significant variability in size and shape, which is a critical factor for understanding the characteristics of teff grain in a positive dilute-phase pneumatic conveying system.

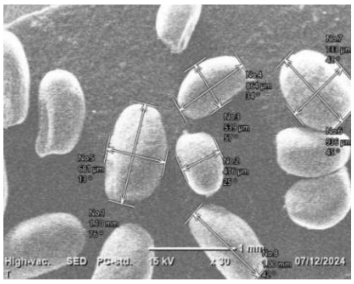

Fig. 4. (a) SEM image X30 (b) SEM image X60 (c) SEM image X270

Table 1. Summary of measured teff grain dimension

Teff Variety	Width (mm)	Thickness (mm)	Length (mm)	Moisture content
Boset	0.63±0.05	0.56+0.10	1.01±0.13	9%-16%
Felagot	0.52±0.07	0.52+0.08	0.92±0.08	8%-14%

Twenty pieces of teff seeds were used for dimension measurement, where dimensions of each seed: length L (mm), width W (mm), thickness T (mm) were determined and the geometric mean diameter Dg = 0.68mm and arithmetic mean diameter Da = 0.72mm were calculated as shown in Eqs. (1-2) and Figure 5. The geometric and arithmetic mean are expressed as follows [29].

$$D_g = \sqrt[3]{W \times T \times L} \tag{2}$$

$$D_a = \frac{W + T + L}{3} \tag{3}$$

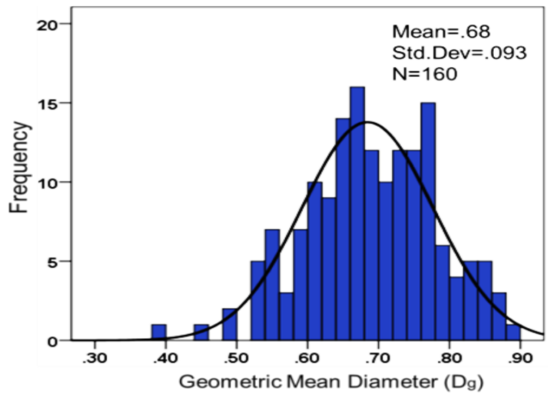

(a)

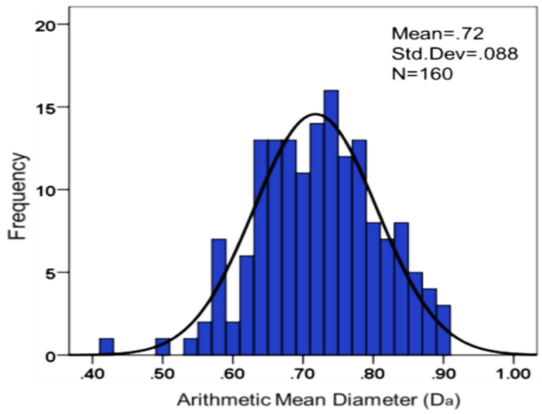

(b)

Fig. 5. (a) Geometric mean diameter and (b) arithmetic mean diameter

Densities of two varieties were measured at different moisture contents. Particle size in diameter (Dp), bulk density and true density for Felagot (DZ-Cr-442 RIL77C) and Boset (DZ-Cr-409) bulk and true density were calculated by the following expression [30].

$$\rho_b = \frac{W}{V} \tag{4}$$

Where ρ_b = bulk density (kg/m^3), W = total mass (kg) and V = total volume (m^3).

$$\rho_t = \frac{W}{V_t} \tag{5}$$

where ρ_t = true density (kg/m^3), W = total mass (kg) and V = true volume(m^3).

$$\varepsilon = \left(1 - \frac{\rho_b}{\rho_t}\right) \times 100 \tag{6}$$

where ε = the porosity (%), ρ_b = the bulk density (kg/m^3), and ρ_t = the true density (kg/m^3).

In addition to dimensional analysis, an electronic balance was used to measure teff-grain thousand-grain weight with a precision of 0.01 mg. Reliable measurements are essential for understanding the mass variations among the grains due to moisture content. The results from these laboratory measurements are summarized in Table 2, which provides detailed data on the dimensions and thousand-grain weights of teff grain.

Table 2. Densities of teff grain

Teff variety	Bulk density (kg/m^3)	True density(kg/m^3)
Boset	779.93-855.23	981.54-1057.04
Felagot	782.02-825.07	996.19-1136.80

Teff grain was prepared by sieving and drying in the oven to test for different moisture content and filled in CEL-MKII Fixed and Fluidized Bed Apparatus Air one and Air two at the height of the bed of 300mm for both varieties. The compressor was connected to the apparatus, and data were transferred to a computer with installed (CEL -MKII fixed and fluidized software). The air flow-rate valve was opened gradually by little increment until the pressure drop was unchanged. The results were recorded by computer (CEL -MKII fixed and fluidized software) as shown in Figure 6.

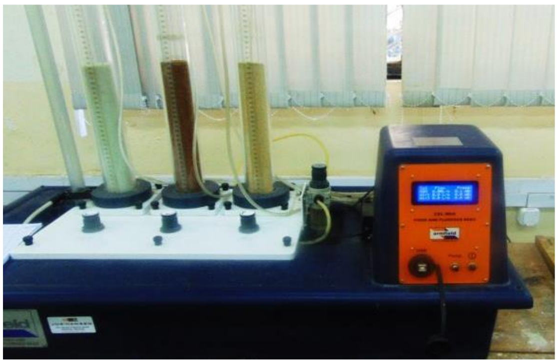

(a)

(b)

(c)

Fig. 6. (a) CEL-MKII Fixed and Fluidized Bed Apparatus , (b) air flow control unit and (c) monitor

The fluidized bed laboratory test used the Carman Kozeny equation expressed in Eq. (7), to predict the minimum fluidization velocity and pressure drop [31].

$$\frac{\Delta P}{L}\cdot\frac{D_p}{\rho(U_{mf})^2}\cdot\frac{\varepsilon^2}{1-\varepsilon}=150\frac{1-\varepsilon}{R\varepsilon}+1.75 \qquad (7)$$

The pressure drop (ΔP) is determined by several factors, including the minimum fluidization velocity or superficial air velocity (U_{mf}), the size of the granules (D_p) measured in meters (here, 0.68 mm), and the original height of the bed (L) in meters (0.3 m in this case). Additionally, the viscosity of air (μ_a) is given as 10^{-5} Ns/m^2, while the kinematic viscosity of air (v_a) is 10^{-6} m^{2}s^{-1}. The density of air (ρ_a) and the granule density (ρ) are also key parameters, both measured in kg/m^3. Finally, the bed voidage (ε) plays a crucial role in calculating the pressure drop. Together, these variables influence the fluidization behavior of the granular bed.

Re=Average Reynolds' number based on Superficial velocity ($D_p.U_{mf}.$ ρ/μ) which is dimensionless. If the flow rate Q is measured in liters/second, and Ufm is the average superficial velocity in ms-1, then:

$$U_{mf}=\frac{Q\times10^{-3}}{A} \qquad (8)$$

where A = Bed cross-sectional area (Bed diameter = 0.05 m).

3. Results and Discussions

The data from laboratory tests was used to create the graph, which displayed the relationship between superficial gas velocity, pressure drop, and bed height.

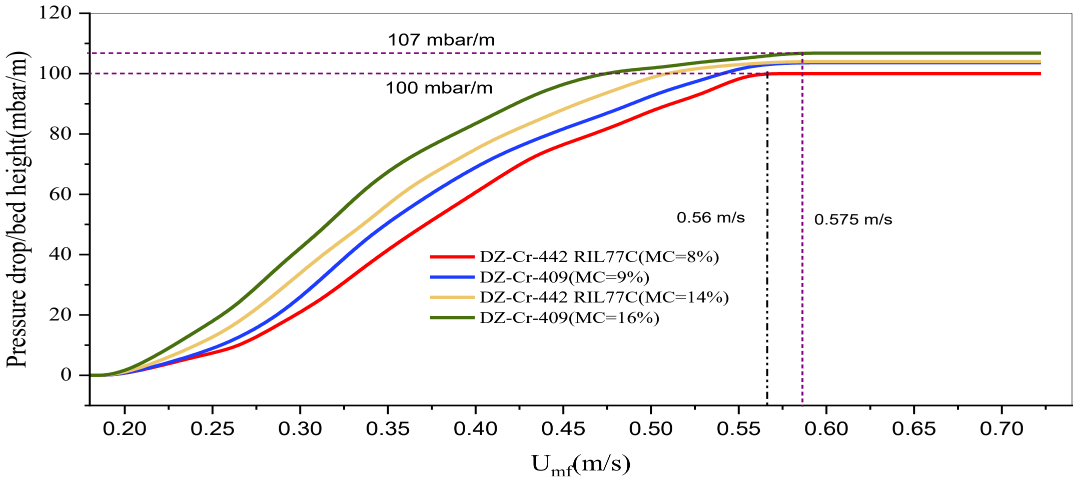

Fig. 7. Minimum fluidization velocity (m/s) vs. pressure drop/bed height (mbar/m) for teff grain

Figure 7 highlights the fluidization characteristics for two varieties of teff grain (DZ-CR-442 RL77C, and DZ-Cr-409) with varying moisture levels. Minimum fluidization velocity ranges from 0.56 to 0.575 m/s, while the pressure drop ranges from 100 to 107 mbar/m. These results indicate that the Boset variety demonstrates slightly higher fluidization velocities and pressure drop/bed height.

Classification of Teff grain as a Geldart Group B particle is key to understanding how it behaves when conveyed pneumatically. This group designation signifies free-flowing material that fluidizes with bubbles. Knowing this helps determine important factors in conveying systems, such as the air speed needed to start fluidization, pressure changes, and how the particles interact with the air. Figure 8 illustrates the laboratory observations of bubble formation in a fluidized bed of teff grains at varying air velocities.

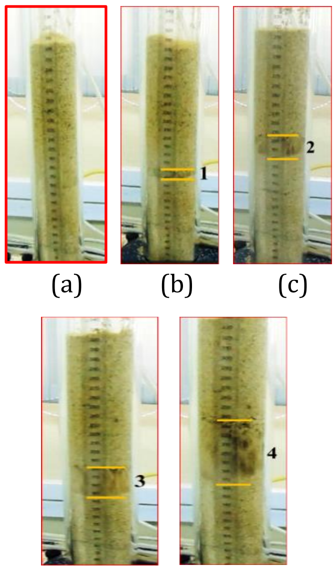

(a) (b) (c) (d) (e)

Fig. 8. (a) fixed bed, (b) bubble formed, (c) bubbles growth, (d) moderate bubble and unstable bed formed and (e) large bubble formed and grains start to move from apparatus

The process begins with the initial attempt of bubble formation (Figure 8a), followed by the creation of small bubbles at position 1 (Figure 8b). As airflow increases, bubbles continue to grow at position 2 (Figure 8c), developing into larger bubbles at position 3 (Figure 8d), and eventually forming very large bubbles at position 4 (Figure 8e). The findings indicate that teff grains generate bubbles at low air velocities, a phenomenon that persists until the pressure drop stabilizes. As airflow increases, the pressure drop rises, creating disturbances within the bed. Once the pressure drop stabilizes, airflow moves through the bed, causing suspension of the grains, which eventually exit the apparatus.

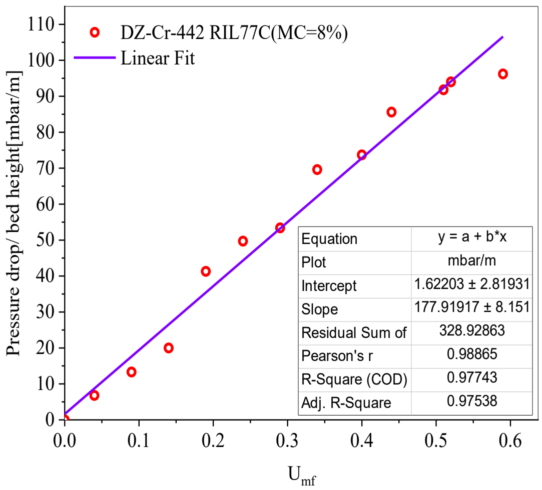

Fig. 9. Minimum fluidization velocity (m/s) air velocity vs. pressure drop/bed height for DZ-Cr-442 RIL77C (MC=8%)

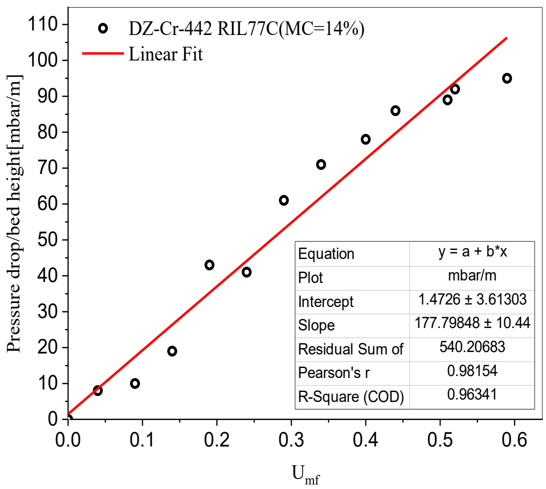

Fig. 10. Minimum fluidization velocity (m/s) air velocity vs. pressure drop/bed height for DZ-Cr-442 RIL77C (MC=14%)

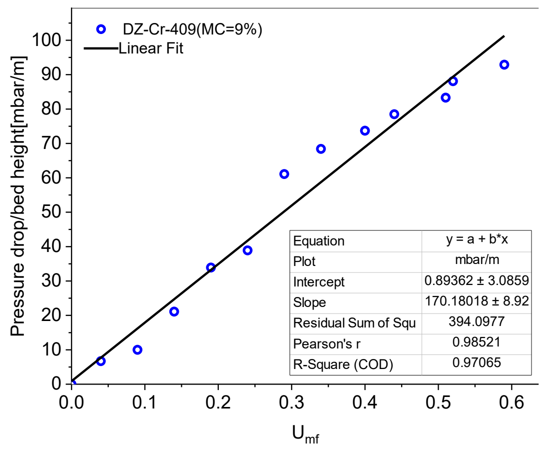

Fig. 11. Minimum fluidization velocity (m/s) air velocity vs. pressure drop/bed height for DZ-Cr-409 (MC=9%)

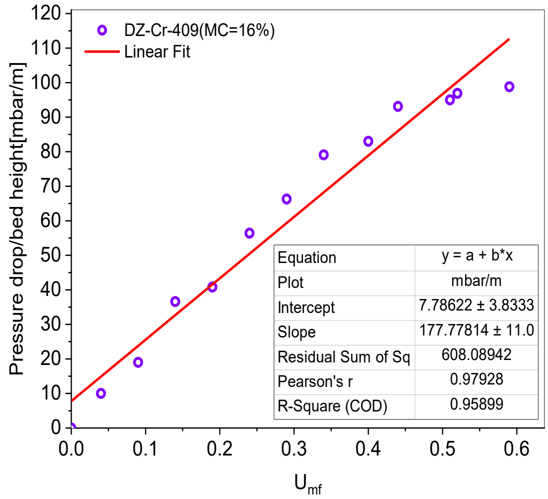

Fig. 12. Minimum fluidization velocity (m/s) air velocity vs. pressure drop/bed height for DZ-Cr-409 (MC=16%)

Figures 9-12 show the correlation between minimum fluidized bed air velocity and pressure drop up to the point where superficial air velocity (minimum fluidized bed air velocity) was achieved or the point where pressure drop remained unchanged. The laboratory test results provided minimum fluidized air velocity and pressure drop per bed height for two varieties of teff grain: DZ-Cr-442 RIL77C at a moisture content of 8%-14% and DZ-Cr-409 at a moisture content of 9%-16%. Based on the findings, researchers and designers used to design and develop efficient teff grain drying and pneumatic conveying systems.

The relationship between minimum fluidization velocity and pressure drop/bed height reveals the influence of teff grain variety and moisture content.

DZ-Cr-442 RIL77C (MC = 8%) shows the highest correlation (R^2= 0.975), indicating highly predictable fluidization behavior, while DZ-Cr-442 RIL77C (MC = 14%) has a slightly lower correlation (R^2 = 0.963), suggesting minor variations with increased moisture. DZ-Cr-409 (MC = 9%) maintains a strong correlation (R^2 = 0.970), similar to DZ-Cr-442 RIL77C at 8%, whereas DZ-Cr-409 (MC = 16%) has the lowest correlation (R^2 = 0.958), indicating that higher moisture may slightly affect fluidization due to increased inter-particle cohesion or density changes.

Despite these variations, the consistently high R^2 values confirm the reliability of experimental data.

Table 3. Analysis of variance

ANOVA					
Source	The sum of Squares (SS)	Degrees of Freedom (df)	Mean Square (MS)	F-value	p-value
Moisture Content (MC)	1125.6	3	375.2	58.4	< 0.001
Variety	420.3	1	420.3	65.4	< 0.001
Residuals	313.5	63	4.98		
Total	1859.4				

The ANOVA results show that both moisture content (MC) and teff grain variety significantly affect gas fluidization characteristics, particularly pressure drop per bed height (mbar/m) (See Table 3)

Moisture content has a highly significant effect ($p < 0.001$) with an *F*-value of 58.4, indicating a strong influence on fluidization behavior.

The sum of squares (1125) suggests that moisture content plays a dominant role in determining pressure drop.

Higher moisture levels likely increase grain cohesion, making fluidization more difficult and leading to higher pressure drops.

Similarly, teff grain variety also has a significant effect ($p < 0.001$, F = 65.4), indicating that different varieties exhibit distinct fluidization behaviors. These differences may arise due to variations in grain size, shape, or surface characteristics, which affect airflow resistance and fluidization efficiency.

The residual variance is relatively small (SS = 313.5), suggesting that the model explains most of the observed variability. These findings have practical implications for industrial applications such as drying, pneumatic conveying, and separation, where understanding the effects of moisture content and grain variety can help optimize processing conditions.

The regression analysis results in Table 4 highlight a high degree of model accuracy and reliability across all tested conditions. The R^2 values, which range from 0.995 to 0.998, confirm an excellent model fit, suggesting that more than 99.5% of the variance in the response variable is explained by the model. This implies that the models effectively capture the underlying relationships in the data, leaving minimal unexplained variation.

Table 4. Regression analysis

Metric	DZ-Cr-442 (14%)	DZ-Cr-442 (8%)	DZ-Cr-409 (16%)	DZ-Cr-409 (9%)
R^2	0.997	0.996	0.998	0.995
MSE	4.23	5.81	2.67	7.94
RMSE	2.06	2.41	1.63	2.82
MAE	1.72	1.98	1.29	2.31
MAPE (%)	2.41%	2.89%	1.68%	3.15%
Relative MSE	0.004	0.006	0.003	0.008
Relative MAE	0.017	0.020	0.013	0.023
CV (%)	2.12%	2.45%	1.69%	2.91%

The Mean squared error (MSE) and root mean squared error (RMSE) values are low across all cases, with RMSE ranging from 1.63 to 2.82. These values indicate that prediction errors are minimal. Notably, DZ-Cr-409 (16%) has the lowest RMSE (1.63), suggesting that this condition yields the most precise predictions among the tested scenarios.

Similarly, the mean absolute error (MAE) and mean absolute percentage error (MAPE) values are consistently low, with MAPE remaining below 3.2% for all cases. This suggests that relative errors are small, further confirming the model's accuracy. Additionally, the relative MSE and Relative MAE values are minimal, reinforcing the robustness of the predictions.

The Coefficient of variation (CV %), which measures error relative to the mean, is below 3% for all conditions, indicating a stable and reliable model. Overall, these results demonstrate that the regression models provide highly accurate predictions of fluidization behavior for different teff grain varieties and moisture levels. Among them, DZ-Cr-409 (16%) exhibits the best predictive performance, with the lowest RMSE, MAE, and MAPE values.

4. Conclusions

Classification of teff grain as a Group B particle according to the Geldart classification is crucial to understanding its pneumatic conveying behavior. This designation indicates that teff grain is readily fluidized with characteristic bubbling. This knowledge directly impacts key parameters like minimum fluidization velocity and pressure drop within conveying systems, as well as the fundamental interactions between the teff particles and the conveying air.

The experimental results highlight the significant impact of moisture content on the minimum fluidization velocity and pressure drop for different teff grain varieties. For instance, the Boset variety (DZ-Cr-409) and Felagot variety (DZ-Cr-442 RIL77C) showed that the fluidization behavior of the teff grain is a critical factor in designing efficient pneumatic conveying systems. Based on the Geldart classification of particles, teff is categorized under Group B material, characterized as medium-sized and medium-density particles. Such particles typically exhibit bubbly fluidization behavior, making it more suitable for dilute-phase pneumatic conveying rather than dense-phase conveying. The bubbly nature of the teff grain in the bed can lead to turbulent flow in dense-phase pneumatic conveying systems, resulting in high-pressure drops and also causing sudden blockages of the system. Experimental studies revealed that bubbles form in the fluidized bed at the minimum superficial gas velocity, with a pressure drop ranging between 100 mbar/m and 107 mbar/m and a minimum fluidization velocity of 0.56 m/s to 0.575 m/s. Therefore, teff grain is better suited for dilute-phase pneumatic conveying systems, as dense-phase conveying leads to operational inefficiencies due to its inherent fluidization characteristics.

The study demonstrates that both moisture content and teff grain variety significantly influence gas fluidization characteristics. Additionally, differences in grain variety contribute significantly to fluidization behavior, likely due to variations in grain size and shape. The model effectively captures these effects, with a small residual variance, confirming its reliability. These findings provide valuable insights for optimizing industrial processes such as drying, pneumatic conveying, and separation of teff grain.

Nomenclature

Symbol	Description
A	Bed cross-sectional area (m^2)
D	Bed diameter (m)
D_a	Arithmetic mean diameter(mm)
D_p	Size of granules (m)
D_g	Geometric mean diameter (mm)
w	Wet weight (kg/m^3)
d	Dry weight (kg/m^3)
U_{mf}	Minimum fluidization velocity (m/s)
l	Original height of bed (m)
Re	Average Reynolds number (-)
Δp	Pressure drop (Pa)
Q	Air flow rate (l/s)
W	Width (mm)
T	Thickness (mm)
L	Length (mm)
N	Number of samples (-)

Greek letters

ρ	Granule density (kg/m^3)
ρ_a	Density of air (kg/m^3)
ρ_b	Bulk density (kg/m^3)
ρ_t	True density (kg/m^3)
ε	Bed voidage (-)
μ_a	Dynamic viscosity of air ($N \cdot s/m^2$)
ν_a	Kinematic viscosity of air (m^2/s)

Subscripts

a	Air
mf	Minimum fluidization
g	Geometric

p	Granules
t	True
b	Bulk

Abbreviations

MC	Moisture content
Std.Dev	Standard Deviation
EIAR	Ethiopian Institute of Agricultural Research
DZARC	Debre Zeit Agricultural Research Center

Funding Statement

This research did not receive any specific grant from funding agencies in the public, commercial, or not-for-profit sectors.

Conflicts of Interest

The author declares that there is no conflict of interest regarding the publication of this article.

Authors Contribution Statement

Lemi Demissie Boset: Conceptualization, Investigation, Reviewing, Writing Original Draft and Editing;

Zewdu Abdi Debele: Conceptualization, Analysis, Visualization and Supervision;

Amana Wako Koroso: Analysis, Reviewing and Supervision.

References

[1] Abdissa, B., Math, R., Desham, K., and Korra, S., 2020. Moisture sorption behavior and shelf life prediction of teff seed and flour. *Journal of Applied Packaging Research*, 12(1), p. 1.

[2] Gonite, T. and Reda, H., 2018. Design and prototyping of teff (ጤፍ) row planter and fertilizer applier. *International Journal of Mechanical Engineering and Applications*, 6(4), p.91.

[3] Tiguh, E.E., Delele, M.A., Ali, A.N., Kidanemariam, G., and Fanta, S.W., 2024. Assessment of harvest and postharvest losses of teff (Eragrostistef (Zucc.)) and methods of loss reduction: A review. *Heliyon*, 10(9).

[4] Debebe, S. 2022. Post-harvest losses of crops and its determinants in Ethiopia: tobit model analysis. *Agriculture & food security*, 11(1), pp.1-8.

[5] Sen, K., Ghosh, S., and Sarkar, B., 2017. Comparison of customer preference for bulk material handling equipment through fuzzy-AHP approach. *Journal of The Institution of Engineers (India): Series C*, 98(3), pp.367-377.

[6] Karimi, M., Moradi, M., Niakousari, M., and Karparvarfard, S.H., 2022. Application of heat carrier particles in a fluidized bed dryer: Dimensionless modeling and GHG emissions. *Journal of Food Process Engineering*, 45(9), p.e14071.

[7] Pontawe, R.J., Asuncion, N.T., Villacorte, R.B., and Martinez, R.C., 2016. Pilot-scale fluidized bed drying system for complete drying of paddy. *PHilMech Technical Bulletin*, 6(1).

[8] Cheng, S., Skylas, D.J., Whiteway, C., Messina, V., and Langrish, T.A., 2023. The effects of fluidized bed drying, soaking, and microwaving on the phytic acid content, protein structure, and digestibility of dehulled faba beans. *Processes*, 11(12), p.3401.

[9] De Munck, M.J.A., Dullemond, M., Peters, E.A.J.F., and Kuipers, J.A.M., 2023. Experimental gas-fluidized bed drying study on the segregation and mixing dynamics for binary and ternary solids. *Chemical Engineering Journal*, 465, p.142756.

[10] Askarishahi, M., Salehi, M.S., and Radl, S., 2023. Challenges in the simulation of drying in fluid bed granulation. *Processes*, 11(2), p.569.

[11] Liu, Z., Du, B., Zhao, W., Li, X., Li, J., Bu, C., and Yi, H., 2009, February. Effect of characterization of powder on particle velocity in dense-phase pneumatic conveying. *In Journal of Physics: Conference Series* (Vol. 147, No. 1, p. 012068). IOP Publishing.

[12] Cheng, S., Skylas, D.J., Whiteway, C., Messina, V., and Langrish, T.A.G. 2023. The effects of fluidized bed drying, soaking, and microwaving on the phytic acid content, protein structure, and digestibility of dehulled faba beans. *Processes*, 11(12), doi: 10.3390/pr11123401.

[13] de Munck, M.J.A., Peters, E.A.J.F., and Kuipers, J.A.M. 2023. CFD-DEM fluidized bed drying study using a coarse-graining technique, Ind. *Eng. Chem. Res.,* 62(48), pp. 20911–20920, doi: 10.1021/acs.iecr.3c02960.

[14] Alkassar, Y., Agarwal, V.K., Pandey, R.K., and Behera, N., 2021. Analysis of dense phase pneumatic conveying of fly ash using CFD including particle size distribution.

Particulate Science and Technology, 39(3), pp.322-337.

[15] Lu, Y., Zhao, L., Han, Q., Wei, L., Zhang, X., Guo, L., and Wei, J., 2013. Minimum fluidization velocities for supercritical water fluidized bed within the range of 633–693 K and 23–27 MPa. *International Journal of Multiphase Flow*, 49, pp.78-82.

[16] Singh, R.K., Dhaigude, N.D., Sahu, A., Chauhan, V., Sahu, G., Saha, S., and Chavan, P.D., 2023. Significance of temperature and pressure on minimum fluidization velocity in a fluidized bed reactor: An experimental analysis. *Energy Sources, Part A: Recovery, Utilization, and Environmental Effects*, 45(1), pp.1793-1806.

[17] Yehuda, T. and Kalman, H. 2020. Geldart classification for wet particles. Powder Technology, 362, pp. 288–300, doi: 10.1016/j.powtec.2019.11.073.

[18] Tavares, R., Santana, Dias C., Rodrigues Moura, C.H., Rodrigues, E.C., Viegas, B., Macedo, E., and Estumano D.C., 2022. Parameter Estimation in Mass Balance Model Applied in Fixed Bed Adsorption Using the Markov Chain Monte Carlo Method. *Journal of Heat and Mass Transfer Research*, 9(2), pp.219-232.

[19] Ayawei, N., Ebelegi, A.N., and Wankasi, D., 2017. Modelling and interpretation of adsorption isotherms. *Journal of Chemistry*, 2017(1), p.3039817.

[20] Tavares, R.S., Dias, C.S., Moura, C.H.R., Rodrigues, E.C., Viegas, B., Macedo, E., and Estumano, D.C., (2022). Parameter estimation in mass balance model applied in fixed bed adsorption using the Markov chain Monte Carlo method. *Journal of Heat and Mass Transfer Research*, 9(2), pp. 219–232.

[21] Anantharaman, A., Cocco, R.A., and Chew, J.W., 2018. Evaluation of correlations for minimum fluidization velocity (Umf) in gas-solid fluidization. *Powder technology*, 323, pp.454-485.

[22] Hideo, I., Husain, S., Akihiko, H., and Naoto, H., 2007. Heat and mass transfer analysis of fluidized bed grain drying. Memoirs of the Faculty of Engineering, Okayama University, 41(1), pp.52-62.

[23] Dhillon, B., Wiesenborn, D., Dhillon, H., and Wolf-Hall, C., 2010. Development and evaluation of a fluidized bed system for wheat grain disinfection. *Journal of Food Science*, 75(6), pp.E372-E378.

[24] Hideo, I., Husain, S., Akihiko, H., and Naoto, H., 2007. Heat and mass transfer analysis of fluidized bed grain drying. Memoirs of the Faculty of Engineering, Okayama University, 41(1), pp.52-62.

[25] Ali, M., Mahmud, T., Heggs, P.J., Ghadiri, M., Djurdjevic, D., Ahmadian, H., de Juan, L.M., Amador, C., and Bayly, A., 2014. A one-dimensional plug-flow model of a counter-current spray drying tower. *Chemical Engineering Research and Design*, 92(5), pp.826-841.

[26] Güner, M.E.T.I.N., 2007. Pneumatic conveying characteristics of some agricultural seeds. *Journal of Food Engineering, 80(3)*, pp.904-913.

[27] Chan, Y., Dyah, T.N., and Kamaruddin, A., 2015. Solar dryer with pneumatic conveyor. *Energy Procedia*, 65, pp.378-385.

[28] Zewdu, A.D. and Solomon, W.K., 2007. Moisture-dependent physical properties of tef seed. *Biosystems Engineering*, 96(1), pp.57-63.

[29] Boset, L.D., Debele, Z.A., and Koroso, A.W., 2024. Pressure Drop Due to Cyclone Separator in Positive Dilute Phase Pneumatic Teff Grain Conveyor. *Journal of Applied Fluid Mechanics*, 18(2), pp.317-331.

[30] Tsegaye, G.A., and Abera, S., 2020. The study of some engineering properties of teff [Eragrostis teff (Zucc.) Trotter] grain varieties. *International Journal of Food Engineering and Technology*, 4(1), p.9.

[31] Li, G., Li, X.S., and Li, C., 2017. Measurement of permeability and verification of Kozeny-Carman equation using statistic method. *Energy Procedia*, 142, pp. 4104-4109.